The impact of specialized enemies on the dimensionality of host dynamics

Ottar N. Bjørnstad*†, Steven M. Sait‡, Nils C. Stenseth§, David J. Thompson‡ & Michael Begon‡

** National Center for Ecological Analysis and Synthesis, 735 State Street, Suite 300, Santa Barbara, California 93101-3351, USA*
‡ Population and Evolutionary Biology Research Group, School of Biological Sciences, University of Liverpool, PO Box 147, Liverpool L69 3BX, UK
§ Division of Zoology, Department of Biology, University of Oslo, PO Box 1050 Blindern, N-0316 Oslo, Norway

Although individual species persist within a web of interactions with other species, data are usually gathered only from the focal species itself. We ask whether evidence of a species' interactions be detected and understood from patterns in the dynamics of that species alone. Theory predicts that strong coupling between a prey and a specialist predator/parasite should lead to an increase in the dimensionality of the prey's dynamics, whereas weak coupling should not. Here we describe a rare test of this prediction. Two natural enemies were added separately to replicate populations of a moth. For biological reasons that we identify here, the prediction of increased dimensionality was confirmed when a parasitoid wasp was added (although this increase had subtleties not previously appreciated), but the prediction failed for an added virus. Thus, an imprint of the interactions may be discerned within time-series data from component species of a system.

Interactions between various natural enemies and their insect prey or hosts represent some of the tightest links in ecological systems[1,2]. In particular, predominantly specialist enemies may induce coupled host–enemy dynamics[3]: the abundance of the host species is affected by the abundance of the enemy, which in turn feeds back on the abundance of the host. This dynamic coupling may greatly alter an ecological system's persistence and dynamics[1–3]. The feedback loop in coupled systems, moreover, generates a delay or lag in the regulation of the host[4,5]. Thus, theory predicts that an added specialist enemy should result in an increase in the number of lags necessary to explain host dynamics when host dynamics are expressed as a function of host densities at various times in the past[4–6]. The number of lags or the 'order of density dependence' (the 'embedding dimension' of the systems' dynamics) reflects the number of functionally different interacting groups[6–8]. Because different life stages of a single species may be functionally distinct, and interactions between different species may be weak, the order need not equate to the number of species present. Thus, as the number of species in a system increases, the 'ecological dimension' (the number of functional groups capable of interacting) increases necessarily, but the dimension of the dynamics need not.

Here we report a direct empirical examination of this relationship between the ecological dimension and the dynamical dimension (the order of density dependence). We added two different natural enemies to laboratory populations of the Indian meal moth (*Plodia interpunctella*): the *P. interpunctella* granulovirus (PiGV) and the parasitoid wasp, *Venturia canescens*. The dimensionality of the dynamics was estimated by nonlinear time-series analysis. We also combine statistical and mathematical modelling to investigate how coupling (or its absence) can be detected in individual time series of the component species of a system, and explore the nature of any changes in dimensionality that may occur.

The study system: basic dynamics

Laboratory cultures of *P. interpunctella* have been studied both experimentally[2,9–11] and theoretically[12–15]. Replicated host, host–pathogen and host–parasitoid populations were maintained for about two years (Fig. 1). The parasitoid adults typically lay their eggs singly in third to fifth instar host larvae[16,17], within which they develop and finally kill the host. Parasitoid larvae synchronize their development with that of their host, and adults emerge 21–25 days after parasitization[18]. PiGV is a baculovirus that is transmitted through host larval ingestion of virus when either infected cadavers or contaminated medium are eaten[19,20]. Resistance to infection increases with age: the fifth (final) instar is effectively invulnerable. Overt disease leads to host death, but sublethal effects include reduced fecundity and prolonged development[9–11,15].

In host-alone populations, dead adult moths, pupae and larvae

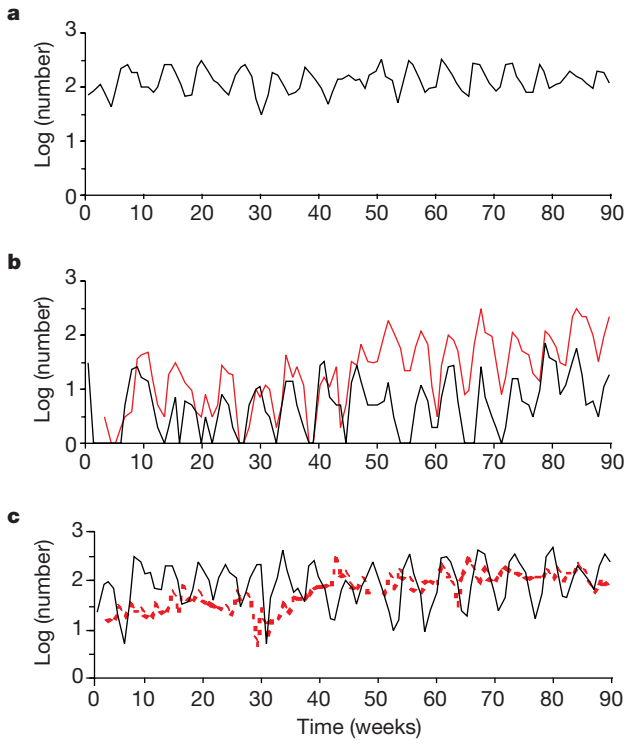

Figure 1 Abundances of the host (thin black line). **a**, Alone; **b**, in the presence of the *Venturia canescens* parasitoid (solid red line); **c**, in the presence of the *Plodia interpunctella* granulovirus (PiGV; dotted red line). The series show representative replicates of each treatment for the first 90 weeks of the experiment.

† Present address: Department of Entomology, 501 ASI building, Penn State, University Park, Pennsylvania 16802, USA.

were counted weekly. In host–parasitoid populations, established by adding two parasitoids 14 days after the initial host population had mated, adult wasps were also counted. In host–virus populations, PiGV-infected larvae were added at the same time as the host, and both uninfected and infected larvae (the unit of observation for the virus) were thereafter counted[2,9–11,16,17]. All time series of the host have dominant periodic behaviour in the 6–7-week range (Table 1). The mean and variability (as measured by the coefficient of variation) of the host in the host–virus system are comparable to those of the host when alone, although the range and amplitude of the cycles are slightly greater (Fig. 1). The host–parasitoid system, in contrast, exhibits greatly depressed host abundance and more violent fluctuations. Furthermore, the period of the fluctuations is slightly shorter (Table 1).

Coupling strengths and dynamic dimensions

The dimension (and order of the density dependence) of each time series was estimated using the nonparametric method of Tong and co-workers[21–23], modified to avoid any spurious effects of serial correlations between nearby points in the time series (see Box 1). As determined in previous work[15], the most parsimonious time-series model of the host-alone dynamics is of dimension three (Fig. 2); and, contrary to expectation for coupled enemy–host interactions, there is no evidence of the dimension increasing in the presence of the virus. For the host–parasitoid replicates, however, the dimensions of both the host and the parasitoid series are five—which is conspicuously higher than that of the host when alone or with the virus (Fig. 2; see Box 1). Five gives a significantly better fit than three for these systems, whereas three is significantly superior to five in the host-alone and the host–virus systems (Fig. 2).

The contrast in the dimension of the dynamics is explicable in terms of the different coupling strengths of the virus and parasitoid to the host. To show this, we estimate the nature of the coupling between the different species through nonparametric regression for abundance data[6,15,24,25] (Fig. 3) using general forms of conventionally accepted functions for all interactions (see Methods). The natural enemy developmental periods are around 3 weeks for both the *Plodia*–*Venturia*[18] and the *Plodia*–PiGV systems[9–11]. The functions were estimated (see Methods) using a two-dimensional smoothing spline with four degrees of freedom (to avoid making *a priori* assumptions about the functional forms for which we wish to test) and a negative binomial error[25]. These regression analyses reveal that the number of adult parasitoids emerging is an increasing function of both the numbers of susceptible larvae and adult parasitoids present 3 weeks earlier (Fig. 3a). Whereas the number of adult hosts decreases rapidly with previous parasitoid abundance, the number increases with host larval abundances (Fig. 3b). This paired set of properties establishes that the parasitoid–host system is fully coupled.

Whereas the number of PiGV-infected larvae is an increasing function of both the number of susceptible larvae and the infected larvae present 3 weeks earlier (Fig. 3c), the number of adult hosts does not decrease with the abundance of previously infected host larvae (Fig. 3d). Thus, the host–virus system is not fully coupled. Enhanced host abundance leads to increased pathogen incidence, but this increase does not feed back negatively on the host. This lack of host–virus coupling is surprising because the virus is a highly specialized enemy that induces significant mortality in the early larval instars of the host[9–11]. (The alternative hypothesis of a strong virus effect on the host that is hidden because of fast virus dynamics (within a host generation) was considered, but rejected because the virus-infected cadavers (not the virus particles) are the functional unit for transmission[19,20].)

The explanation for the unaltered host dimension lies in the strong competition between large larvae[15]. In contrast to the parasitoid, which attacks older larvae, the virus is most infectious to younger larvae, and so the virus-induced mortality can be partially compensated for through the life cycle of the host. This is not to say that the virus fails to affect the host dynamics. Indeed, previous studies show that it alters host demography to exaggerate the fluctuations[15]. Nevertheless, this virus fails to engage in coupled enemy–host dynamics.

Stage-structure and significant lags

To interpret further the dimension of the dynamics, we develop a simple stage-structured scheme of the interactions[15] (see Box 2). This scheme predicts a three-dimensional model for the host alone (with lags in regulation of 1 week, 3 weeks and 6 weeks), but a five-dimensional model for the host–parasitoid interaction (with additional lags at 4–5 weeks and 7–8 weeks). The three lags in the host-alone model reflect (1) a density-dependent (and negative) interaction at a lag of around 1 week, generated by competition and

Table 1 Summary of the experimental time series

Replicate	Species	*n*	Mean	Coefficient of variation ($CI_{95\%}$)	Period
PV1	*P. interpunctella*	130	12.1	229% (189,262)	40.5
	V. canescens	127	43.9	147% (122,168)	–*
PV2	*P. interpunctella*	130	8.2	140% (117,162)	42.8
	V. canescens	127	52.2	119% (102,136)	42.8
PV3	*P. interpunctella*	77	6.2	163% (129,199)	43.5
	V. canescens	74	24.1	126% (105,150)	43.5
PP1	*P. interpunctella*	74	155.5	79% (67, 89)	47.2
	PiGV	73	69.5	100% (84,114)	47.2
PP2	*P. interpunctella*	88	151.9	77% (62, 90)	43.3
	PiGV	87	73.4	68% (53, 78)	43.3
PP3	*P. interpunctella*	91	137.0	81% (70, 92)	45.8
	PiGV	90	85.2	67% (57, 77)	–
P1	*P. interpunctella*	95	105.6	62% (52, 70)	44.3
P2	*P. interpunctella*	48	108.2	73% (59, 87)	52.5
P3	*P. interpunctella*	108	132.4	59% (52, 66)	45.0

PV1–PV3 signify the three host–parasitoid replicates (*P. interpunctella* is the host, *V. canescens* is the parasitoid). PP1–PP3 signify the three host–virus replicates (*P. interpunctella* is the host, PiGV is the virus infected larvae). P1–P3 signify the three host-alone replicates. *n*, total length of the time series; mean, average abundance; coefficient of variance denotes 100s.d./mean, where s.d. is the standard deviation. 95% Confidence intervals ($CI_{95\%}$) are calculated by bootstrapping the series (with 10,000 resamples). Period denotes the dominant period in the periodogram (in weeks).
* Subdominant period: 38.5 days.

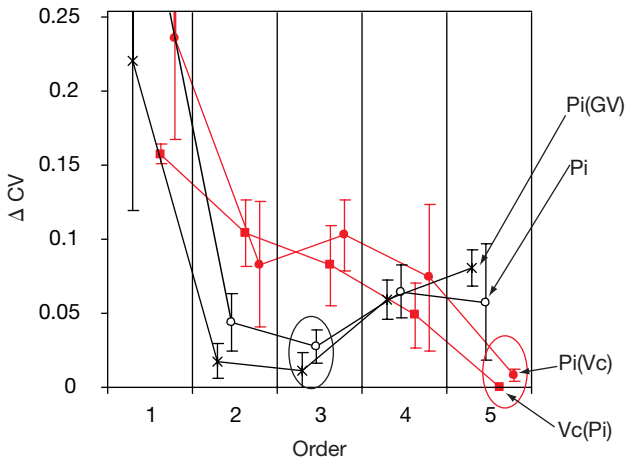

Figure 2 Cross-validation for the order of density dependence according to the method of Tong and co-workers[21–23] (Box 1). Cross-validation error is plotted against order for each of the three treatments. Shown are the cross-validation profiles for *P. interpunctella* (Pi), the host alone; Pi(Vc), the host in the presence of the parasitoid; Pi(GV), the host in the presence of the virus; Vc(Pi), the parasitoid in the presence of the host. For each replicate, the cross-validation error was calculated relative to the optimal order. ΔCV represents the average loss in predictive ability across all replicates. The error bars represent one standard error. The parsimonious orders (circles) are three for the host alone and the host in the presence of the virus, but five for the host–parasitoid interaction. See Supplementary Information for details.

cannibalism of large larvae on small; (2) a second density-dependent interaction at a lag of around 3 weeks, generated by competition amongst small larvae and cannibalism of large larvae on eggs; and (3) a positive term at a lag of around one host generation (~6 weeks), representing host reproduction (but discounted by intra-stage competition).

The host–parasitoid model predicts the dimension to increase by two, but the delayed density-dependent structure contributes a total of five new terms to the host dynamics (Box 2). Three of these take the same form: the dependences predicted by the host-alone model, discounted by the rate (μ_p) at which parasitoid attack rate (in the vicinity of the equilibrium) increases with increasing parasitoid abundance. Each of these terms appears about 2 weeks later in the new model as compared with the original term. Two weeks is the approximate delay between the peak period of parasitoid attacks, on the largest host larvae, and the time when unparasitized hosts would have emerged as adults[9–11]). Thus, we see—three times—the loss of hosts to parasitoids leading to a dilution of the interactions in the host-alone model. There is less reproduction, less competition and less cannibalism because there are fewer hosts, as a result of their having been attacked by adult parasitoids present ~2 weeks previously.

The fourth addition further discounts the host reproduction term (lag 6). Thus, discounting because of losses of larvae is now attributable not only to intra-stage competition (as in the host-alone model), but also because increased abundance of larvae leads to increased parasitoid attack rates.

Finally, the fifth term, operating with a 1-week lag, appears to describe the effect of survival against parasitoid attack, as it enters in the form $A_t = \mu_p A_{t-1}$, where A_t represents the number of adult moths at time t (Box 2), that is, μ_p here is a survival rate. Moreover, because μ_p is low when parasitoids experience intense 'interference' at equilibrium but is high when they do not, the term appears also to capture, as predicted by theory[26], the potentially damping effects

Box 1

Time-series estimates of the order

Royama[4] developed the theory for the interrelation between the dynamical dimension and the order of density dependence of an ecological time series. This order may therefore be studied when trying to understand the dynamics of a system[5,8]. The classical estimation of the order of a time series relies on the goodness of fit of linear models of various complexities[35]. However, several alternative methods have been proposed in order not to constrain analyses to be valid only for roughly linear dynamical systems. We estimate the order of each time series according to the order-consistent, nonparametric method of Tong and co-workers[21–23]. This method does not require assumptions about linearity (or any other functional form, except the assumption of smoothness[36]) and uses cross-validation of the locally linear regression against lagged abundances to estimate the expected future abundance on the basis of a population's trajectory. The candidate nonparametric model that presupposes the correct order will be the best at forecasting, and will thus minimize the cross-validation error[21]. As there is fairly strong correlation between adjacent observations and this may induce spurious results[37], we remove a whole generation (7 weeks, that is, 3 weeks at each side of the target week) during the cross-validation (see Methods). Pooling across replicates, dimension 5 was a significantly better fit to the data than dimensions 1–4 for the time series of host with parasitoid (and parasitoid with host) (Fig. 2), whereas for host alone and host with virus, dimension 3 was the best fit—significantly better than dimensions 1, 4 and 5 for the host–virus systems, and than dimensions 1 and 4 for the host alone.

Testing the method

The order-consistent nonparametric method is known to provide correct estimates of the order of long time series[21–23]. Whether it is possible to identify high orders correctly from the type of data obtained in ecological studies, however, is unknown. We therefore undertook an analysis of the power of the method when applied to time series from three well known age-/stage-structured ecological models representing many dimensional complexities. In each instance, we simulate the models for 150 time steps and discard the first 50 observations. The resulting time series—of comparable length (100 observations) to the replicates analysed above—are subjected to identical analyses to those of the real data. The simplest model is a (non-age-structured) one-dimensional stochastic Ricker model[38]. The second model is the three-dimensional LPA-model for the stage-structured dynamics of the flour beetle[30]. The third model is the SR model for fish stock/recruitment dynamics[31], in which the dimension can be anywhere from two to four depending on the number of age classes. (See Methods for details of the models and parameters used.)

The figure shows the cross-validation (CV) profiles across 25 realizations of each model. For the Ricker model (**a**), the order is correctly identified as 1 in most cases. Note that the bars represent standard deviations and not standard errors. Furthermore, the order is correctly identified as 3 in most cases of the LPA model (see figure), and as 2, 3, and 4, respectively, in the SR model (**b**). In the Supplementary Information we detail results for a wide range of model parameters for each of the three sample models. The overall conclusions of the simulation are that the nonparametric method can correctly identify the order (of at least up to four) of time series from diverse ecological systems on the basis of 100 observations. The order tends to be biased upwards for highly nonlinear versions of the models. The order is at most increased by one, however, and the fit of the larger model is only very marginally better (by ΔCV around 0.01)

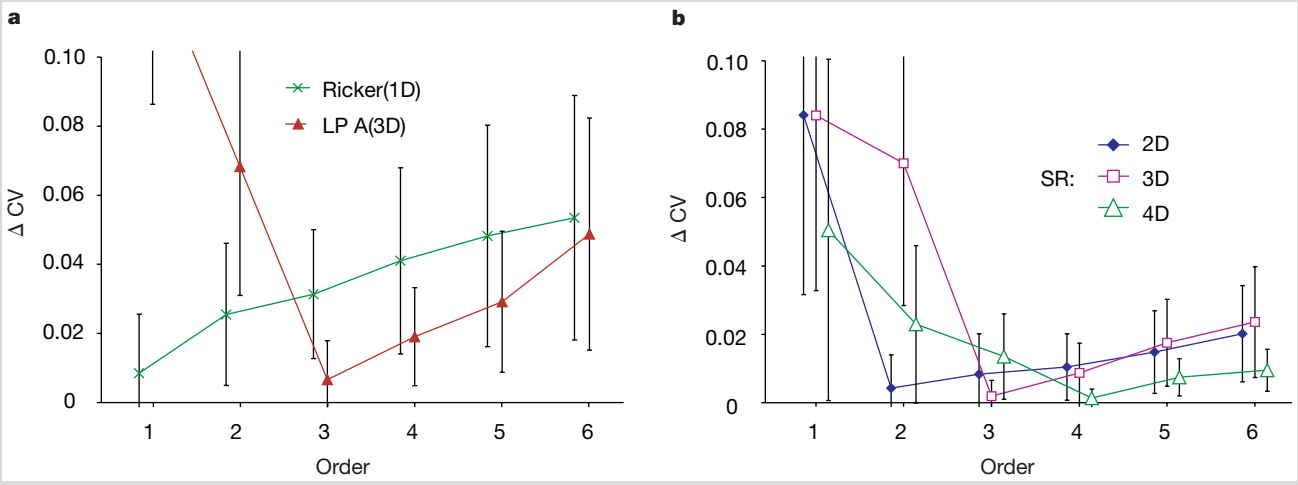

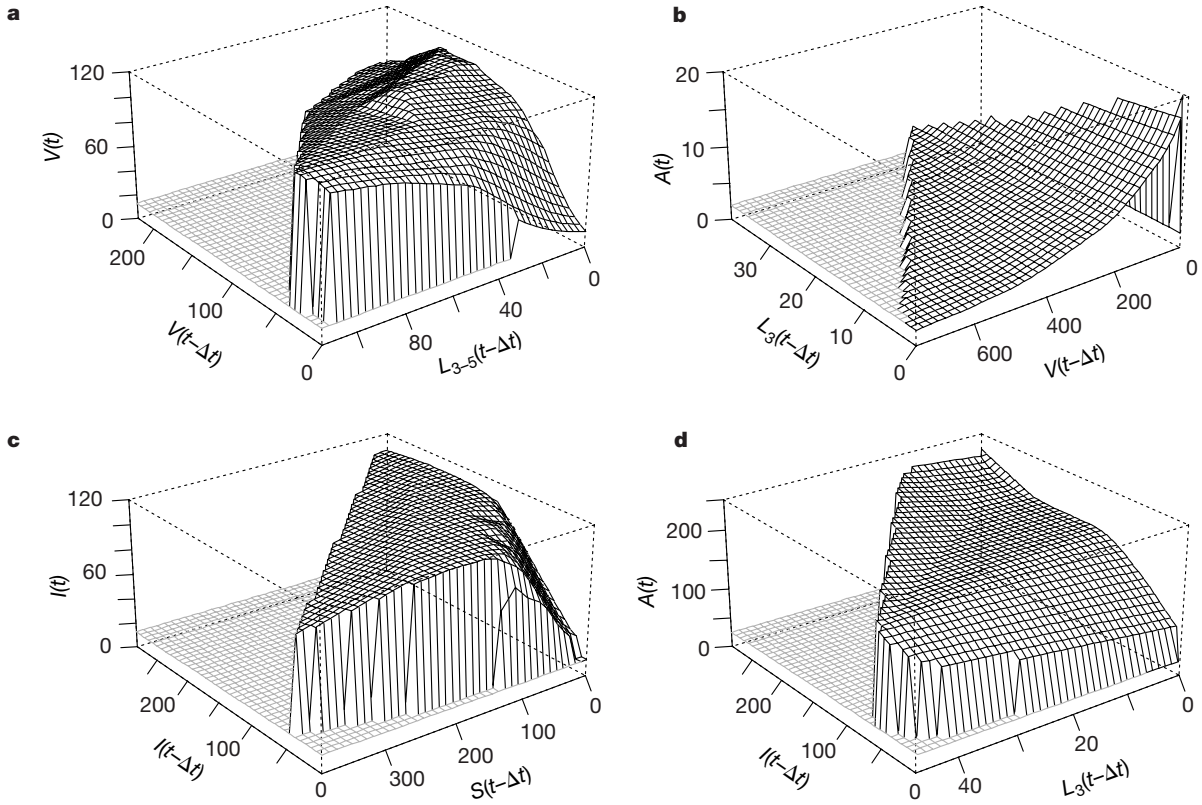

Figure 3 The estimated functions. **a**, Abundance of adult parasitoids, V, as a function of the number of parasitoids and susceptible host larvae (instar 3–5), L_{3-5}, 3 weeks previously (function H in Methods). **b**, Abundance of adult hosts, A, versus abundance of host (instar 3) larvae, L_3, and the three parasitoid cohorts that may attack them 3 weeks previously (function K in Methods). **c**, Abundance of granulovirus-infected larvae, I, versus the number of infected larvae and susceptible larvae (instar 1–4), S, 3 weeks previously (function F in Methods). **d**, Abundance of adult hosts, A, versus abundance of host (instar 3) larvae, L_3, and infected larvae 3 weeks previously (function G in Methods). We estimate the functions by using a two-dimensional smoothing spline. All functions are statistically significant at a nominal 1% level (see Methods). The grey-shaded grids along the xy-planes signify states for which no data are available and to which no functions are fitted.

on dynamics of parasitoid attack acting without a delay: more parasitoid interference leads to more immediate (as opposed to delayed) feedback on host dynamics.

Thus, the move from three to five dimensions in the presence of the parasitoid turns out not simply to be a case of the original hosts' three dimensions being supplemented by two new host–parasitoid dimensions. Instead, more subtly, there appears to be a combination of direct, trophic effects (entirely new terms) and indirect, modulating effects (modifications of existing terms, sometimes with a time delay). The new terms sometimes increase the dimensionality but at other times do not.

Furthermore, there is compelling evidence within the time-series data themselves for the precise lag structures predicted by the stage-structured models. Using Wald tests[27] (see Methods), highly significant lags are detected in the host data from the host–parasitoid series at lags of 1, 3, 4–5, 6 and 7–8 weeks. In contrast, host series when alone or in the presence of the virus exhibit highly significant lags at 1, 3 and 6 weeks, but no evidence of lagged regulation at 4–5 or 7–8 weeks. This striking congruence between data and models reinforces our confidence in the results of both the mechanistic predictions and the statistical analyses.

Conclusions

Our results show that specialist enemies can, as theory predicts, increase the dimension of host dynamics through complete coupling (*Venturia–Plodia*), but also that the increase in dimensional complexity can be counterbalanced if coupling is weak (PiGV–*Plodia*). There may be a direct connection in ecological systems between the number of identifiable interacting groups and the dynamic dimension—but such a connection is not inevitable. This helps explain why certain keystone species embedded in rich ecological communities exhibit low-dimensional dynamics[6]. Potentially, it may also illuminate the enigmatic nature of biological control[28]. *Plodia* is a serious stored-food pest[29], and pathogens (such as PiGV) and parasitoids (such as *Venturia*) are prime candidates for its biological control. Although they are both specialist enemies, one (the parasitoid) serves to depress host densities (Table 1) and the other (the virus) is ineffective. The difference in efficiency is related to the way the parasitoid engages in coupled interactions with the host but the virus does not.

Furthermore, our findings show how even when specialist enemies (or other additional species) increase the dynamic dimension of an ecological system, there may be a complex, but tractable, link between the number of added interactants and the number of added dimensions. Finally, we are excited to show that, with appropriate analysis, the imprint of the detailed interactions in a system's dynamics can be discerned from time-series data of a component species. □

Methods

The locally linear regression

A gaussian product kernel was used. The bandwidth of the kernel was also optimized using cross-validation. We carried out the analyses on time series for which the first 20 observations (~3 host generations) were discarded to allow for a transient period. The data were square-root transformed to stabilize the variance. Overall results are given in Fig. 2 and Box 1; for the results for individual replicates, see Supplementary Information.

Ecological models in Box 1

The 'Ricker model' is a one-dimensional model, $N_{t+1} = N_t \exp[r(1 - N_t)]u_t$, where N is

Box 2

A predictive model for dimensional changes

To predict the impact of the parasitoid on the host dynamics, we first develop a model for the host dynamics. We then add parasitoid–host interaction to the model to calculate its effects. We consider the following five stages in the host life-cycle: E, eggs; S, small larvae (consisting of instars 1–3); L, large larvae (consisting of instars 4–5); P, pupae; A, adults. The developmental times between each of these are in the order of (but on average a little longer than) a week (range from 5 to 10 days; see details in ref. 15). Because adults do not require any resources, the number of eggs produced at time t is directly proportional to the number of adults, $E_t = rA_t$, where r is the *per capita* reproduction. For simplicity, we assume the large larvae to be the most important cannibals of eggs and larvae. Thus, survival of eggs may decrease due to density-dependent cannibalism by these. In this way, $S_t = E_{t-1}\Gamma(L_{t-1})$, where Γ is a decreasing function of L_{t-1}. Within-stage competition and cannibalism by larger larvae reduce the survival of small larvae to the next stage: $L_t = S_{t-1}\Lambda(S_{t-1}, L_{t-1})$, where Λ is a decreasing function of both S_{t-1} and L_{t-1}. Assuming competitive dominance of the large larvae, the survival of these depends only on within stage competition. In this way the number of pupae is:

$$P_t = L_{t-1}\Omega(L_{t-1}) \quad (1)$$

where Ω is decreasing in L_{t-1}. For simplicity we assume density-independent adult emergence (at rate c) from the pupae:

$$A_t = cP_{t-1} \quad (2)$$

We can use a Taylor expansion on a log-scale on this set of five life-cycle equations to predict the dimension of the dynamics. We denote intra-stage density dependence within the small larval stage and large larval stage (in the vicinity of the stable or unstable equilibrium) by β_s and β_l, respectively, and the influence of large larvae on eggs and small larvae by γ_e and γ_s, respectively. We can then write a model in delay coordinates as:

$$\begin{aligned}\log A_t = &-\log A_{t-1}[\gamma_s] - \log A_{t-3}[(1-\beta_s)\gamma_e] \\ &+ \log A_{t-6}[rcP^*(1-\beta_s)(1-\beta_l)] + \text{const}\end{aligned} \quad (3)$$

where the asterisk denotes evaluations at the equilibrium, and const represents the collection of constant terms. Equation (3) predicts that life-cycle interactions within the host result in three-dimensional dynamics with lags in regulation at week 1, week 3 and week 6. The exact delays result from considering the duration of each life-stage[15]. The first and second lag reflect cannibalism of small larvae and eggs, respectively. But note that the latter is discounted by within-stage competition. The third lag reflects reproduction (but as modified by intra-stage competition in small and large larvae).

The parasitoid–host interaction

In the presence of the parasitoid we need to modify equations (1) and (2) to take into account that a proportion of the large larvae will become adult parasitoids (see Methods): $V_t = kL_{t-2}\Omega(L_{t-2})h(V_{t-2}, L_{t-2})$. The complementary proportion will escape parasitism and metamorphose into adult hosts $A_t = cL_{t-2}\Omega(L_{t-2})[1 - h(V_{t-2}, L_{t-2})]$. We can use a Taylor expansion (on a log-scale) on this modified set of life-cycle equations to predict the changes to host dimensional complexity when interacting with a parasitoid. We let μ_l and μ_p denote, respectively, how increases in large *Plodia* larvae and increases in adult parasitoid abundance affect the parasitoid attack rate (in the vicinity of the stable or unstable equilibrium). All other symbols are as defined above. The resultant delay coordinate representation is for *Plodia–Venturia*:

$$\begin{aligned}\log A_t = &-\log A_{t-1}\{\gamma_s && -\mu_P\} \\ &-\log A_{t-3}\{(1-\beta_s)\gamma_e && +\gamma_s\mu_P] \\ &-\log A_{t-4/5}\{ && (1-\beta_s)\gamma_e\mu_p\} \\ &+\log A_{t-6}\{rcP^*(1-\beta_s)(1-\beta_l) && -rcP^*(1-\beta_s)\mu_l)\} \\ &-\log A_{t-7/8}\{ && rcP^*(1-\beta_s)(1-\beta_l)\mu_p\} \\ &+\text{const}\end{aligned} \quad (4)$$

Equation (4) is five-dimensional, with the same three lags as equation (3) but with additional lags at 4–5 weeks and 7–8 weeks. A total of five additional terms are induced. In the equation, these are placed in a separate column on the right to aid readability. The model thus predicts an increased dimensionality when the parasitoid was added, though the nature of the increase has several subtleties.

the scaled density, r (= 1.5) is the growth rate, and u is a sequence of log-normal variates with unit mean. In the simulations, we assumed a coefficient of variation of 10%. The 'LPA model' is the three-dimensional larvae–pupae–adult (LPA) model for the dynamics of *Tribolium* flour beetle populations[30]: $L_{t+1} = bA_t \exp[-c_{el}L_t - c_{ea}A_t + E_{1t}]$; $P_{t+1} = L_t(1-\mu_l)$; $A_{t+1} = P_t\exp[-c_{pa}A_t] + A_t(1-\mu_a)$, where b (= 6.6) represents reproduction; c_{el} (= 1.2×10^{-2}), c_{ea} (= 1.2×10^{-2}) are cannibalism rates of eggs by pupae and larvae, respectively; c_{pa} (= 0.05) is adult cannibalism on pupae; and μ_l (= 0.2) and μ_a (= 0.8) are larval and adult mortality rates. E_{1t} is a sequence of normal variates with mean zero and standard deviation 0.35.

The 'SR model' is the stock-recruitment model of fish dynamics that encompasses the interactions between young of the year (X), juveniles (Y) and mature individuals (S)[31]: $X_t = bS_t\alpha_t$; $Y_{t+1} = X_t\exp[-\beta\ln(X_t) - \gamma\ln(Y_t)]$; $S_{t+1} = (1-\mu_y)Y_t + (1-\mu_s)S_t$, where b (= 13) is the reproduction rate, and α is a sequence of log-normal variates (with a mean of 1 and a coefficient of variation 0.3); β and γ are juvenile competition and cannibalism rates; μ_y (= 0.1) and μ_s are juvenile and mature mortality rates. The dimension of the model depends on the mortality rates of the mature individuals, ranging from 2 (when $\mu_s = 1$) to 3 or 4 ($\mu_s < 1$). In the simulation we use $\beta = 0.5$ and $\gamma = 0.4$ when $\mu_s = 1$, and $\beta = 0.3$ and $\gamma = 0.7$ when $\mu_s < 1$. (In the Supplementary Information we consider a wide range of parameter values for each of the three models.)

Virus–host and parasitoid–host coupling

Transmission of the virus is through contact between previously infected larvae, I, and susceptible larvae, S, taken to consist of the first four larval instars. The proportion, $f()$, of susceptible larvae that becomes newly infective in the period from $t - \Delta t$ to t is a function of the abundance of infectives and susceptibles: $I_t = S_{t-\Delta t}f(I_{t-\Delta t}, S_{t-\Delta t}) = F(I_{t-\Delta t}, S_{t-\Delta t})$, where Δt is the time taken for disease development. Full virus–host coupling implies that as virus abundance increases with S, host abundance decreases with I. For strictly lethal infections it should do so. But infection may not necessarily be lethal[9–11,32], so the number of adult *Plodia*, A, can be modelled as $A_t = m_sS_{t-\Delta t}[1 - f()] + em_sS_{t-\Delta t}f() = G(I_{t-\Delta t}, S_{t-\Delta t})$, where m_s is the fraction of uninfected larvae that successfully metamorphose into adults. The subscript s indicates that this fraction may be density dependent. The parameter $(1-e)$ measures virus-induced mortality; m_se is thus the fraction of infected larvae that successfully metamorphose into adults.

'Transmission' of the parasitoid occurs through adult parasitoids (the 'infective stage') ovipositing into susceptible larvae. The number of susceptible larvae, L, consist of larval instars 3–5 (refs 16–18). The number of new adult parasitoids, V, is a function of the abundance of adult parasitoids and susceptible host larvae one development period previously: $V_t = kL_{t-\Delta't}h(V_{t-\Delta't}, L_{t-\Delta't}) = kH(V_{t-\Delta't}, L_{t-\Delta't})$, where $\Delta't$ is the time taken for parasitoid development, and k is the hatching rate of adult parasitoids from parasitized larvae. The function $h()$ governs the proportion of larvae that become parasitized. Classically $h() = 1 - \exp(-mV_{t-\Delta t})$[33], so that $H()$ is typically an increasing function in V and L. Parasitization is usually lethal[18], so the number of adult *Plodia* emerging will be a function of the unparasitized larvae: $A_t = m'_sL_{t-\Delta't}[1 - h()] = K(V_{t-\Delta't}, S_{t-\Delta't})$. The parameter m'_s is the fraction of unparasitized larvae that successfully metamorphose into adults. The subscript s indicates that this fraction may be density dependent.

When we estimated the functions nonparametrically we used two-dimensional smoothing splines with four degrees of freedom[15,25], and a negative binomial error model[25,34]. In Fig. 3, the information is pooled across the three replicates of each treatment[15]. Zero observations in the response (that is no adults observed) were omitted from the analyses because these induced singularities in the estimation. All functions are statistically significant (Fig. 3a: $F_{280,4} = 21.5$, $P < 0.001$; 3b: $F_{286,4} = 5.55$, $P < 0.001$; 3c: $F_{283,4} = 19.1$, $P < 0.001$; 3d: $F_{253,4} = 5.54$, $P < 0.001$). The shape parameter, κ, in the negative binomial is around unity or lower for the *Plodia–Venturia* system (*Plodia* $\kappa = 0.69$, s.e. = 0.07; *Venturia* $\kappa = 1.06$, s.e. = 0.10), and slightly higher than that in the *Plodia*–PiGV system (*Plodia* $\kappa = 1.62$, s.e. = 0.13; PiGV $\kappa = 3.08$, s.e. = 0.26). The results for the individual replicates are near identical to the treatment-wise analysis, although the power is somewhat lower (see Supplementary Information for details).

Testing for significant lags

We use the Wald test[27] to test for significant lags in regulation. A generalized linear model was constructed relating log-abundance to log-abundance at lags: 1, 3, 6, 4–5, and 7–8 for the time series of the host alone and in the presence of the two specialist enemies (Box 2). A

log-link was used and the error was assumed to follow an overdispersed Poisson process[34]. Lags falling between sampling intervals were studied by averaging across the two adjacent sampling intervals (that is, lag 4–5 is taken as average of abundance in the week 4 and week 5 previously). A constant of unity was added to the lagged variables before log-transformation. The results (summarized across the replicates[15]) are as follows: *Plodia*–*Venturia* series: (lag 1: $t = 13.48$, $P < 0.01$; lag 3: $t = -3.03$, $P < 0.01$; lag 4–5: $t = 3.38$, $P < 0.01$; lag 6: $t = 3.37$, $P < 0.01$; lag 7–8: $t = -4.35$, $P < 0.01$); *Plodia*–PiGV series: (lag 1: $t = 2.30$, $P < 0.02$; lag 3: $t = -4.62$, $P < 0.01$; lag 4–5: $t = -0.95$, $P = 0.34$; lag 6–7: $t = 5.58$, $P < 0.01$; lag 7–8: $t = -0.62$, $P = 0.53$); *Plodia* alone series: (lag 1: $t = 3.86$, $P < 0.01$; lag 3: $t = -3.49$, $P < 0.01$; lag 4–5: $t = 0.59$, $P = 0.56$; lag 6: $t = 6.75$, $P < 0.01$; lag 7–8: $t = 0.72$, $P = 0.47$). Note that PiGV increases the generation time of the host by about half a week[15]. The significance of regulation is therefore tested at a lag of 6–7 weeks. The results for the individual replicates are near identical to the treatment-wise average, although the power is somewhat lower (see Supplementary Information for details).

Received 12 October; accepted 29 November 2000.

1. Hassell, M. P. & May, R. M. Generalist and specialist natural enemies in insect predator–prey interactions. *J. Anim. Ecol.* **55,** 923–940 (1986).
2. Begon, M., Sait, S. M. & Thompson, D. J. Predator–prey cycles with period shifts between two- and three-species systems. *Nature* **381,** 311–315 (1996).
3. Murdoch, W. W. & Stewart-Oaten, A. Predation and population stability. *Adv. Ecol. Res.* **9,** 1–131 (1975).
4. Royama, T. *Analytical Population Dynamics* (Chapman & Hall, London, 1992).
5. Turchin, P. Rarity of density dependence or population regulation with lags? *Nature* **344,** 660–663 (1990).
6. Stenseth, N. C., Falck, W., Bjørnstad, O. N. & Krebs, C. J. Population regulation in snowshoe hare and lynx populations: asymmetric food web configurations between the snowshoe hare and the lynx. *Proc. Natl Acad. Sci. USA* **94,** 5147–5152 (1997).
7. Schaffer, W. M. Ecological abstraction: The consequence of reduced dimensionality in ecological models. *Ecol. Monogr.* **51,** 383–401 (1981).
8. Berryman, A. A. *Population Systems: a General Introduction* (Plenum, New York, 1981).
9. Sait, S. M., Begon, M. & Thompson, D. J. Long-term population dynamics of the Indian meal worm moth *Plodia interpunctella* and its granulosis virus. *J. Anim. Ecol.* **63,** 861–870 (1994).
10. Sait, S. M., Begon, M. & Thompson, D. J. The influence of larval age on the response of *Plodia interpunctella* to a granulosis virus. *J. Invert. Pathol.* **63,** 107–110 (1994).
11. Sait, S. M., Begon, M. & Thompson, D. J. The effect of a sublethal baculovirus infection in the Indian meal moth, *Plodia interpunctella*. *J. Anim. Ecol.* **63,** 541–550 (1994).
12. Gurney, W. S. C., Nisbet, R. M. & Lawton, J. H. The systematic formulation of tractable single-species population models incorporating age structure. *J. Anim. Ecol.* **52,** 479–495 (1983).
13. Gurney, W. S. C. & Nisbet, R. M. Fluctuation periodicity, generation separation, and the expression of larval competition. *Theor. Popul. Biol.* **28,** 150–180 (1985).
14. Briggs, C. J., Sait, S. M., Begon, M., Thompson, D. J. & Godfray, H. C. J. What causes generation cycles in populations of stored product moths? *J. Anim. Ecol.* **69,** 352–366 (2000).
15. Bjørnstad, O. N. *et al.* Population dynamics of the Indian meal moth: demographic stochasticity and delayed regulatory mechanisms. *J. Anim. Ecol.* **67,** 110–126 (1998).
16. Sait, S. M. *et al. Venturia canescens* parasitizing *Plodia interpunctella*: host vulnerability – a matter of degree. *Ecol. Entomol.* **20,** 199–201 (1995).
17. Sait, S. M., Begon, M., Thompson, D. J., Harvey, J. A. & Hails, R. S. Factors affecting host selection in an insect host–parasitoid interaction. *Ecol. Entomol.* **22,** 225–230 (1997).
18. Harvey, J. A., Harvey, I. F. & Thompson, D. J. Flexible larval growth allows use of a range of host sizes by a parasitoid wasp. *Ecology* **75,** 1420–1428 (1994).
19. Boots, M. Cannibalism and the stage-dependent transmission of a viral pathogen of the Indian meal moth, *Plodia interpunctella*. *Ecol. Entomol.* **23,** 118–122 (1998).
20. Knell, R. J., Begon, M. & Thompson, D. J. Transmission of *Plodia interpunctella* granulosis virus does not conform to the mass action model. *J. Anim. Ecol.* **67,** 592–599 (1998).
21. Cheng, B. & Tong, H. On consistent nonparametric order determination and chaos. *J. R. Statist. Soc. B* **54,** 427–449 (1992).
22. Cheng, B. & Tong, H. Orthogonal projection, embedding dimension and sample size in chaotic time series from a statistical perspective. *Phil. Trans. R. Soc. Lond. A* **348,** 325–341 (1994).
23. Yao, Q. & Tong, H. Quantifying the influence of initial values on non-linear prediction. *J. R. Statist. Soc. B* **56,** 701-725 (1994).
24. Ellner, S. P. *et al.* Noise and nonlinearity in measles epidemics: Combining mechanistic and statistical approaches to population modeling. *Am. Nat.* **151,** 425–440 (1998).
25. Bjørnstad, O. N., Fromentin, J.-M., Stenseth, N. C. & Gjøsaeter, J. A new test for density-dependent survival: the case of coastal cod populations. *Ecology* **80,** 1278–1288 (1999).
26. Free, C. A., Beddington, J. R. & Lawton, J. H. Inadequacy of simple-models of mutual interference for parasitism and predation. *J. Anim. Ecol.* **46,** 543–554 (1977).
27. Sokal, R. R. & Rohlf, F. J. in *Biometry 1* Ch. XIX, 887 (W. H. Freeman, New York, 1995).
28. Murdoch, W. W. & Briggs, C. J. Theory of biological control: recent developments. *Ecology* **77,** 2001–2013 (1996).
29. Tabashnik, B. E. & McGaughey, W. H. Resistance risk assessment for single and multiple insecticides: Responses of Indian meal moth (Lepidoptera: Pyralidae) to *Bacillus thuringiensis*. *J. Econ. Entomol.* **87,** 835–841 (1994).
30. Costantino, R. F., Desharnais, R. A., Cushing, J. M. & Dennis, B. Chaotic dynamics in an insect population. *Science* **275,** 389–391 (1997).
31. Bjørnstad, O. N., Fromentin, J.-M., Stenseth, N. C. & Gjøsaeter, J. Cycles and trends in cod population. *Proc. Natl Acad. Sci. USA* **96,** 5066–5071 (1999).
32. Grenfell, B. T. & Dobson, A. P. Ecology of infectious diseases in natural populations. (Cambridge Univ. Press, Cambridge, 1995).
33. Nicholson, A. J. & Bailey, V. A. The balance of animal populations. *Proc. Zool. Soc. Lond.* **3,** 551–598 (1935).
34. Venables, W. N. & Ripley, B. D. in *Modern Applied Statistics with S-plus* 1–462 (Springer, New York, 1994).
35. Wei, W. W. *Time Series Analysis* (Addison Wesley, California, 1989).
36. Green, P. J. & Silverman, B. W. in *Nonparametric Regression and Generalized Linear Models: a Roughness Penalty Approach* Ch. 1-IX, 182 (Chapman & Hall, London, 1994).
37. Ellner, S. & Turchin, P. Chaos in a noisy world: New methods and evidence from time-series analysis. *Am. Nat.* **145,** 343–375 (1995).
38. Ricker, W. E. Stock and recruitment. *J. Fish. Res. Board Canada* **11,** 559–623 (1954).

Supplementary information is available on *Nature*'s World-Wide Web site (http://www.nature.com) or as paper copy from the London editorial office of *Nature*.

Acknowledgements

Funding was received from the National Center for Ecological Analysis and Synthesis (O.N.B.) (a Center funded by the NSF, the University of California Santa Barbara and the State of California), from the Norwegian National Science Foundation (O.N.B., N.C.S.) and from NERC (M.B., S.M.S. and D.J.T.). P. Amarasekare, A. Dobson and B. Grenfell commented on the manuscript.

Correspondence and requests for materials should be addressed to O.N.B. (e-mail: onb1@psu.edu).